Materials Science-Poland, 40(4), 2022, pp. 158-170
http://www.materialsscience.pwr.wroc.pl/
DOI: 10.2478/msp-2022-0049

Microplasma-sprayed multilayer coatings for electric heating elements

Sergii Kaliuzhnyi[1], Darya Alontseva[2,*], Sergey Voinarovych[1], Oleksandr Kyslytsia[1], Aleksandr Khozhanov[2], Leszek Łatka[3], Zulfat Faizrakhmanov[2], Gulsym Bektasova[4]

[1]Department of Protective Coatings, E.O. Paton Electric Welding Institute, National Academy of Sciences of Ukraine, 11 Kazymyr Malevich Street, Kyiv 03150, Ukraine

[2]School of Information Technologies and Intelligent Systems, D. Serikbayev East Kazakhstan Technical University, 69 Protozanov Street, Ust-Kamenogorsk 070004, Kazakhstan

[3]Department of Metal Forming, Welding and Metrology, Faculty of Mechanical Engineering, University of Science and Technology, Wrocław 50370, Poland

[4]Department of Physics, Faculty of Natural Sciences and Technology, S.Amanzholov East Kazakhstan University, 30 Gvardeiskya St., Ust-Kamenogorsk 070002, Kazakhstan

The paper presents new results on the application of microplasma spraying (MPS) for manufacturing electric heating elements (EHEs) consisting of a St3 steel plate (the substrate) with a sprayed electrically insulating Al_2O_3 sublayer (400±50 μm thick) and TiO_2 electric heating tracks (4 mm width; 150±50 μm thickness). Measurements of the temperature of the multilayer coating with a thermal imager enabled determination of the temperature distribution over the surface of the EHE. The electric strength and conductivity tests showed the efficiency of the sprayed EHEs up to a temperature of 200°C. The results of analysis of the causes of material losses during MPS of electric heating tracks (TiO_2) are presented, and the optimal parameters for efficient MPS of coatings in the form of narrow tracks on steel substrates are determined. Using regression analyses, the equation for the influence of MPS parameters on the coating transfer efficiency (CTE) is obtained. Process parameters such as the electric current and the plasma-forming gas flow rate have been found to have the greatest influence on the CTE. In the experiment, a high efficiency of the sprayed material during MPS of electric heating tracks of TiO_2 powder was established (the maximum CTE reached 89%), which indicates the prospects for using MPS technology in the production of EHEs for DC electric heating and for maintaining the temperature of product surfaces up to 200°C.

Keywords: *microplasma spraying, electric heating element, multilayer coatings, coating transfer efficiency*

1. Introduction

Electrical heaters are widely used in household and industrial applications. In the household, electric heaters such as electric stoves, irons, electric water heaters, electric boilers, and so on are widely used. In industry, electric heaters are used for heating chemical solutions, metal processing furnaces, heating cabinets, and control stations; in the manufacture of fan heaters; and so on. The main part of the electric heater is the electric heating element (EHE). The following requirements are imposed on materials used in the industrial production of EHEs: good electrical resistance, combined with a low coefficient of linear thermal expansion, and good heat resistance. The most common industrial EHEs are made from iron–chromium–nickel and nickel–chromium alloys with high electrical resistivity. The use of these materials in EHE makes it possible to operate the EHEs up to temperatures of 1,200–1,300°C. The next class of higher-temperature EHEs are commercially available cylindrical heaters made of semiconductor ceramic materials, such as SiC or $MoSi_2$ [1]. Heaters of this type are used for heating to higher temperatures of 1,500–1,700°C, compared with metal heaters. Other ceramic materials with semiconducting properties, such as ZrO_2, TiO_2, TiC, Cr_3C_2, and $LaCrO_3$, have also found application in the manufacture of EHEs [2].

* E-mail: dalontseva@ektu.kz

© Kaliuzhnyi et al. 2022. This is an open access article distributed under the Creative Commons Attribution-NonCommercial-NoDerivatives 4.0 License. (http://creativecommons.org/licenses/by-nc-nd/4.0/)

The widespread use of semiconductor ceramic materials is due to the higher resistivity and lower coefficient of linear thermal expansion of ceramics compared to metals. The relationship between the structure (grain size, chemical and phase compositions, and porosity) and some electrical properties (resistivity; Hall and Seebeck coefficients) in composite ceramics ($(ZnO)_z[(TM)_xO_y]_{1-z}$), where TM = transition metals Fe and Co, is currently being investigated, and the temperature dependence of electrical resistivity ρ (T), as well as the Hall and Seebeck coefficients of emerging donor centers, have been shown, which makes it possible to obtain ceramics with controlled values of resistivity [3].

A design feature of metal EHEs is the need for electrical insulation of the conductive coil from the heated surface. The air gap is mainly used as an electrical insulator. This design of metal EHEs leads to a decrease in the heat transfer coefficient, heat dissipation into the surrounding space, complication of the design, and an increase in the overall dimensions of the EHE, which – in some cases – affects its further installation. To increase the heat transfer coefficient and reduce the dimensions of electric heaters, it is possible to use EHE in the form of electric heating coatings (tracks) deposited directly on the heated surface [4]. As noted above, the electrical properties of coatings depend on their microstructure [3], and recently, technologies have been developed that make it possible to obtain coatings with the required microstructure and properties [5]. In particular, Zhao et al. [6] have developed a functional electric heating coating with a positive temperature coefficient (PTC) by adding multiwall carbon nanotubes into polyurethane/paraffin composites. The coating allows automatic control of the maximum temperature during heating, thus protecting the composite substrate with low temperature resistance and saving electrical energy. The ability to control the temperature has been tested in electrical heating experiments, and the PTC phenomenon has been explained by the microstructural transition model.

Titanium dioxide (TiO_2) is a promising material for use in EHE in terms of its electrical properties. TiO_2 has the properties of a semiconductor with a melting point about 1,850°C; it has been successfully used in electronics, mechanical engineering, and other industries, and today, it is the most affordable semiconductor ceramic material on the market [7]. The successful application of the semiconductor properties of TiO_2 in the fabrication of EHEs is confirmed by the results of Scheitz et al. [8] and Li et al. [9].

Ceramic-based materials are used as electrical insulating materials. Well-known representatives of such materials are Al_2O_3, ZrO_2, and Cr_2O_3; among them, Al_2O_3 is the most widespread. Its use is due to its high dielectric properties at elevated temperatures (up to 9 $kV \cdot mm^{-1}$) [10] and its low cost. The effect of simultaneous additions of Cr_2O_3 and TiO_2 on the microstructure and, accordingly, the electrical properties of aluminum oxide coatings obtained by atmospheric plasma spraying (APS) has been noted by Conzea et al. [7]; the suitability of plasma-$TiOx/Cr_2O_3$ heating coatings for injection molding has also been studied [11].

Currently, electric heating tracks are obtained by such methods as screen printing, spreading, photolithography, vacuum condensation deposition, and so on [5]. Among the existing methods for obtaining electric heating tracks, thermal plasma spraying of coatings is considered a promising technology, in particular, APS, which has advantages such as a wide choice of spray materials and substrates, high productivity, and simplicity of the technological process with the possibility of its automation.

For the first time, the technology of thermal plasma spraying for the manufacture of resistors was applied in 1975 by Smyth and Anderson [12]. Their research was aimed at studying the performance of a mixture of NiO and Fe_3O_4 resistors manufactured by APS. The results of their work showed that the service life of a mixture of NiO and Fe_3O_4 resistors was >10,000 hr at a temperature of 150°C; moreover, the effect of the size of the sprayed particles on the specific resistance of resistors was shown.

Hajaligol et al. [13] – in a US patent – presented the development of an electronic smoking cigarette with a tubular heater. EHEs have been proposed to be produced from a mixture of NiCr-

and NiAl-based powders by APS or high-velocity oxygen fuel (HVOF). The use of EHE in the design of this kind of product has allowed the smoker to pause and restart the tobacco burning process at will, with reduced waste smoke generation.

Michels et al. [14] investigated high-temperature Ni80-Cr20 EHEs fabricated as wide ribbons deposited on solid substrates by plasma spraying techniques such as APS, HVOF, and vacuum plasma spraying (VPS). An electrically insulating ceramic layer was preliminarily applied to the heated surfaces, on which a thin electric heating coating was subsequently formed. Each layer (insulating ceramic and electric heating coating) had a thickness ranging from 75 μm to 300 μm. The EHEs were tested on heat fluxes with power densities up to $17 \cdot 10^6$ $W \cdot m^{-2}$. As a result, it was found that VPS and HVOF electric coatings perform better than APS coatings. This is due to the denser microstructure, better purity, and uniform thickness of the VPS and HVOF coatings.

Prudenziati et al. [15] fabricated EHEs by APS of Ni80-Cr20 coatings with operating temperatures ranging from 20°C to 600°C. However, the problem of stable performance of EHEs manufactured by this method under operating conditions at high temperatures of about 500°C–600°C has not been solved.

Scheitz et al. [8] obtained an EHE with a working heating temperature of 300°C by HVOF and APS of TiO_2 powder both on a flat surface and on a pipe. The EHE had an electric heating coating with a thickness of 100–200 μm. The electrical insulating properties of the coating were provided by the presprayed sublayer of spinel with a thickness of up to 300 μm. The power of the tubular EHE was varied within 540 W at an applied voltage of 60 V.

Based on the results of the study, Scheitz et al. [8] proposed, when applying coatings with electric heating properties, in the future, to use a mixture of 20% Cr_2O_3–80% TiO_2 to increase the operating temperature of the heating process to levels >300°C.

Li et al. [9] presented the results of successful tests of plasma-sprayed electrical heating coatings based on TiO_2 after heat treatment in the cyclic mode with an operating temperature of >300°C.

The prospect of using APS technology in the production of electrically heated coatings is being studied to this day to control the temperature for anti-icing/deicing [16] and to mitigate the accumulation of ice in carbon steel pipes and prevent pipe bursting [17]. However, one of the technological disadvantages that prevent the use of APS for the production of EHEs is the possibility of overheating and distortion of the product as a result of the thermal influence of the plasma jet, as well as large material losses during the spraying of narrow electric heating tracks <6 mm wide.

Losses of sprayed material during APS are caused by splashing and rebound of the sprayed particles, as well as by geometric factors. For example, in conventional plasma-arc spraying, the losses associated with the geometric factor are due to the size of the spray spot diameter (20–25 mm), which is several times greater than the width of the electric heating track (3–5 mm). The loss of material due to spatter and rebound can be characterized by the coating transfer efficiency (CTE). This parameter not only characterizes the efficiency of the process but is also used as an optimization parameter.

Taking into account the need to form thin, narrow electric heating tracks and prevent warping of the substrate, the technology of microplasma spraying (MPS) appears promising. MPS makes it possible to obtain coatings from both metallic and ceramic materials. Due to the small diameter of the spray spot (up to 5 mm), MPS can significantly reduce the loss of the sprayed material, while exerting a minimal thermal effect on the substrate, which makes it possible to obtain coatings on thin-walled parts without warping, as reported by Borisov et al. [18].

The goal of this study was, firstly, to obtain by MPS a small-sized multilayer EHE, consisting of an insulating and an electrically conductive layer, and to measure its functional characteristics, that is, electric strength and conductivity when heated. Secondly, the aim was to evaluate the effectiveness of the application of MPS for the formation of narrow tracks of EHE, that is, to analyze the effect of the size of the sprayed surface and MPS parameters, such as current strength, plasma-forming gas

flow rate, spraying distance, and powder feed rate, on the ETE to provide guidance on selecting optimal EHE spraying parameters and deepen the understanding of MPS processes. Thus, this study focuses on evaluating the effectiveness of using MPS technology for EHE manufacturing, while in a previous paper [18], only the possibility of obtaining EHEs by MPS was shown.

2. Materials and research methods

TiO_2 powder (Metakhim, Moscow, Russia) with a particle size of 15–40 μm was used as a material for obtaining resistive coatings. TiO_2 has a large coefficient of linear thermal expansion (from $8.4{\cdot}10^{-6}$ to $11.8{\cdot}10^{-6}$ K^{-1}), high electrical resistance (from $1.5{\cdot}10^{-8}$ to $1.7{\cdot}10^{-8}$ ohm [19]), good chemical resistance, and good electrical conductivity in oxidizing gas environments, sufficient for resistive self-heating at room temperature, and it is also one of the most affordable semiconductor ceramic materials on the market.

Al_2O_3 powder (Peachim, Kyiv, Ukraine) with a particle size from 20 μm to 63 μm was used to apply electrical insulating coatings. This material was chosen due to its high electrical strength reaching up to 5 $kV{\cdot}mm^{-1}$ [20].

MPS-004 (E.O. Paton Electric Welding Institute, Kyiv, Ukraine) [21] was used as the equipment for MPS of coatings. The parameters of the MPS of electrically insulating and resistive coatings are given in Table 1. The choice of these parameters was based on the analysis of the results of previous studies by the authors [22] and the capabilities of the MPS-004 installation. A previous article [22] presents the results of obtaining Zr coatings with a given porosity of 20% on a Ti6Al4V titanium alloy and substantiates the choice of optimal parameters for efficient spraying of Zr coatings on a steel substrate.

The working surfaces of EHEs with dimensions of 70 mm × 45 mm × 1 mm (Series No. 1) and dimensions of 50 mm × 50 mm × 2 mm (Series No. 2) were made of carbon steel grade St3 (LLC Steel Group, Mariupol, Ukraine), the chemical composition of which is given in Table 2.

Table 1. Parameters of MPS of electrically insulating and resistive coatings

Parameters	**Coating**	
	Al_2O_3	**TiO_2**
Electric current, I (A)	45	40
Voltage, U (V)	30	28
Spraying distance, H (mm)	150	150
Plasma-forming gas (Ar) flow rate, G_{pl} (slpm)	1.3	1.3
Shielding gas (Ar) flow rate, G_{sh} (slpm)	4.0	4.0
Powder feed rate, P_{pow} ($g{\cdot}min^{-1}$)	1.2	2.0

MPS, microplasma spraying; slpm, standard liters per minute

Table 2. Chemical composition of carbon steel St3 according to Ukrainian State Standard DSTU 2651:2005, 2015

Elements	**Wt.% of elements**
C	0.14–0.22
Si	0.15–0.30
Mn	0.40–0.65
Ni	<0.3
Cu	<0.3
Cr	<0.3
As	<0.08
N	<0.008
S	<0.05
P	<0.04
Fe	Balance amount

DSTU, State Standards of Ukraine (*Derzhavni Standarty Ukrainy*)

The gas-abrasive treatment of the working surface was carried out with 95A FARM (Korund, Khimki, Russia) electrocorundum with a grain size of F20–F22 under a compressed air pressure of 7 MPa, followed by a 5-min surface cleaning in an ultrasonic cleaner PS-2 (Jeken, Dongguan, China) unit using isopropyl alcohol.

EHEs were produced by layer-by-layer MPS of Al_2O_3 and TiO_2 powders onto flat steel substrates. The first layer was sprayed with Al_2O_3 powder to provide electrical insulation of the steel substrate from resistive tracks, which were sprayed with TiO_2 powder. To impart a meander shape to the resistive tracks during MPS, masks were applied to the samples: on samples of Series No. 1 of

Table 3. Intervals of variation of the parameters of MPS of electric heating tracks (TiO_2)

Levels of variation	Factors			
	Electric current, I (A)	Plasma-forming gas flow rate, G_{pl} (slpm)	Spraying distance, H (mm)	Powder feed rate, P_{pow} (g·min^{-1})
Upper level +	45	2.0	160	1.8
Lower level –	35	1.0	80	0.6
Base level 0	40	1.5	120	1.2
Variation intervals	5	0.5	40.0	0.6

MPS, microplasma spraying; slpm, standard liters per minute

seven spirals, and on samples of Series No. 2 of six spirals. An additional layer of Al_2O_3 was sprayed on samples of Series No. 2 for external electrical insulation of the electric heating tracks.

The test of the electrical strength of coatings of Al_2O_3 was carried out with a megohmmeter F4102/1 (Uman plant Megaohmmeter, Uman, Ukraine). The measurement of the heating temperature of the electric heating track (TiO_2), in relation to the applied electric voltage, was carried out on a research stand (Figure 1), consisting of an adjustable power supply (U), a switch to interrupt the supply of electric current (K), a UNI-T UT70B (Uni-trend Technology, Dongguan, China) digital multimeter (A and V for measuring the current and voltage, respectively) and an IRISYS 1020 (InfraRed Integrated Systems Ltd., Northampton, UK) thermal imager (T) for measuring the temperature and observing the distribution of heat throughout the EHE.

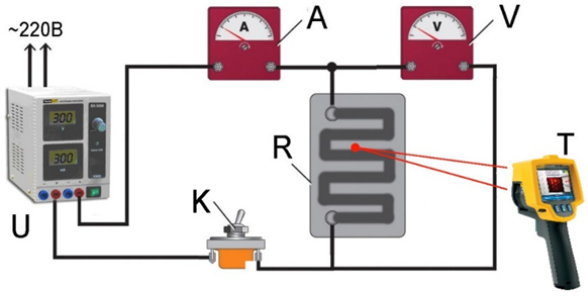


Fig. 1. Scheme of EHE tests: U – regulated power supply; K – switch for interrupting the supply of electric current; A – ammeter; V – voltmeter; R – a sample with an electric heating coating; T – thermal imager. EHE, electric heating element

Studies of the microstructure of microplasma-sprayed electrical insulating and electric heating (resistive) coatings were carried out using a Neophot 32 microscope (Carl Zeiss, Jena, Germany). The porosity was determined by processing images using Image-Pro Plus (Media Cybernetics, Rockville, MD, USA) software in accordance with American Society for Testing and Materials (ASTM) E 2109-01 standard [23]. The evaluation of (i) the efficiency of the MPS process and (ii) the effect of MPS parameters on the microstructure of coatings in the form of narrow resistive heating tracks was carried out using the method of mathematical planning (multifactorial experiment with fractional replicas 2^{4-1}). The intervals of variation of the values of the parameters of the MPS of TiO_2 powder on steel substrates are given in Table 3.

The assessment of the influence of MPS parameters on the CTE was carried out according to the following method. Before MPS, the mass of an uncoated steel substrate was measured on an analytical scale VLR-200 (Gosmetr, St. Petersburg, Russia) with an accuracy of 10^{-5} g. Then, with the stationary plasmatron MPS-004, the TiO_2 powder was sprayed for 15 s with eight different combinations (runs) of spraying parameters according to the plan of the experiments. For the convenience of readers, the MPS parameters for all eight runs are given in the Results and Discussion section, along with the results of the experiments to determine the CTE (Table 4) and with the parameters of the metallization figure (Table 5).

The coating mass (m_c) was calculated as the difference between the masses of the sample after and before MPS. Powder consumption ($m_{p)}$ was determined before each experiment by weighing the amount of powder supplied by the dispenser for

Table 4. The CTE values depending on the parameters of the MPS of TiO_2 powder

Run	I (A)	G_{pl} (slpm)	H (mm)	P_{pow} (g·min^{-1})	CTE, %	
					Experimental	Calculated
1	45	2.0	160	1.8	75	74
2	45	2.0	80	0.6	89	96
3	45	1.0	160	0.6	44	44
4	45	1.0	80	1.8	78	84
5	35	2.0	160	0.6	47	50
6	35	2.0	80	1.8	88	91
7	35	1.0	160	1.8	28	38
8	35	1.0	80	0.6	65	61
9	40	1.5	120	0.8	68	64

CTE, coating transfer efficiency; MPS, microplasma spraying; slpm, standard liters per minute

Table 5. Parameters of the metallization figure depending on the parameters of the MPS of TiO_2 powder

Run	I (A)	G_{pl} (slpm)	H (mm)	P_{pow} (g·min^{-1})	Metallization figure height, h (mm)	Large axis, L (mm)	Small axis, l (mm)
1	45	2.0	200	1.8	2.21	9.2	7.5
2	45	2.0	100	0.6	1.04	6.3	4.7
3	45	1.0	200	0.6	0.53	8.2	7.4
4	45	1.0	100	1.8	2.31	7.2	5.6
5	35	2.0	200	0.6	0.35	8.8	6.2
6	35	2.0	100	1.8	2.27	8.6	6.6
7	35	1.0	200	1.8	0.81	7.2	7.0
8	35	1.0	100	0.6	1.34	7.6	5.4

MPS, microplasma spraying; slpm, standard liters per minute

15 s.

The CTE was calculated using Eq. (1)

$$\text{CTE} = \frac{m_c}{m_p}, \tag{1}$$

where m_c – mass of the coating; m_p – mass of the powder.

To evaluate the effectiveness of the MPS method for the formation of narrow electric heating tracks and analyze the material losses associated with the geometric factor (excessive size of the spray spot in relation to the sprayed area), experiments were carried out to determine the parameters of the metallization figure, which characterizes the mass distribution of the coating material in the spray spot. Metallization figures were obtained by MPS of TiO_2 powder on steel substrates for 10 s in a stationary position of the plasmatron. The resulting metallization figures were measured by determining the dimensions of the vertical (large) L and horizontal (small) l axes of the spray spot, as well as the maximum height h of the sprayed material (Figure 2).

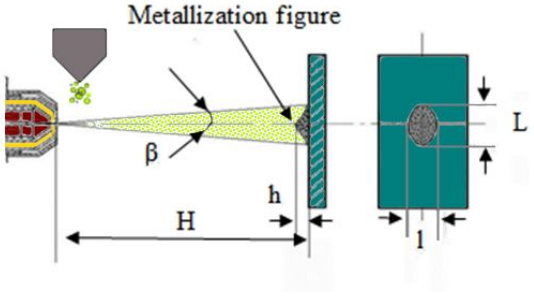


Fig. 2. Scheme for measuring the metallization figure, where H is the spraying distance, β is the opening angle of the plasma jet, h is the height of the sprayed material, L is the vertical (large) axis, and l is the horizontal (small) axis of the spray spot

Using the Olympus 460 (Olympus, Tokyo, Japan) digital camera, the metallization figures were shot in directions perpendicular to their axes, after which the images were processed to determine the coordinates of the profiles of metallization figures. Based on the obtained coordinates, the profiles of metallization figures were constructed in Mathcad (PTC, Montreal, QC, Canada) software environment and the functions describing the profiles were determined for the large and small axes of the spray spot, along which the areas of metallization figures were calculated. An analysis of the profiles of zirconium metallization figures, previously described by the authors [22], showed that the profile of the metallization figures during MPS is reliably described by the Gaussian function or the normal distribution, represented in Eq. (2) [24]:

$$y = y_0 e^{-kx^2}, \tag{2}$$

where y_0 is the maximum height of the metallization figure; k is the numerical coefficient; and x is the width of the profile of metallization figure.

Having data on the dimensions of the metallization figure, the opening angle of the plasma jet β was calculated using Eq. (3):

$$\beta = \left(\frac{L}{2 \cdot H}\right), \tag{3}$$

where L is the vertical (large) axis of the spray spot; H is the spraying distance.

The material loss associated with the geometric factor was determined using Eq. (4):

$$S_{loss} = \left(1 - \frac{S_{x-x}}{S_{tot}}\right) \times 100\%, \tag{4}$$

where S_{tot} is the total area of the metallization figure (Figure 3); isS_{x-x} the area of the metallization figure, limited by the size of the part (see Figure 3).

3. Results and discussion

EHEs fabricated by layer-by-layer MPS of Al_2O_3 and TiO_2 powders on flat steel substrates had electric heating tracks of the following geometric dimensions: the track width was 4 mm, the track length for samples of Series No. 1 was 312 mm, and the track length for samples of Series No. 2 was 295 mm. The appearance of the manufactured multilayer ceramics of series No. 1 and No. 2 are shown in Figure 4.

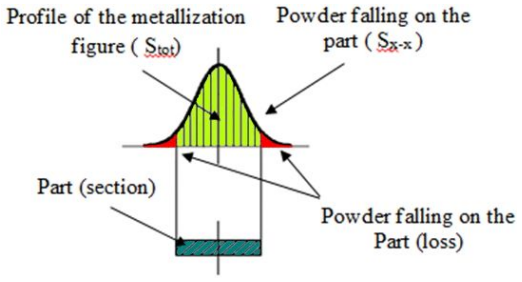
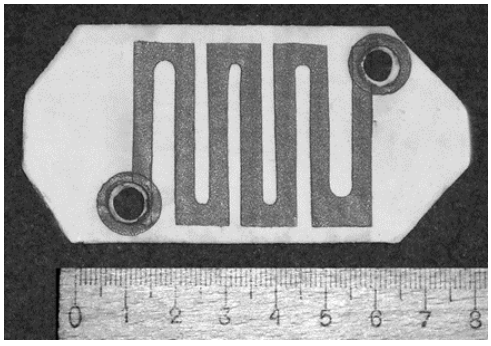
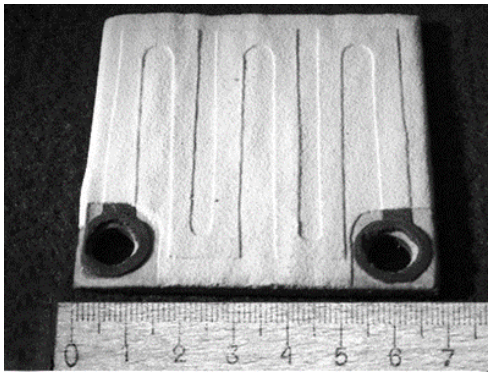


Fig. 3. Diagram explaining the loss of material due to the geometric factor



(A)



(B)

Fig. 4. EHE appearance: (**A**) EHE Series No 1: two-layer coating of Al_2O_3 and TiO_2; (**B**) EHE Series No. 2: three-layer coating of Al_2O_3 and TiO_2. EHE, electric heating element

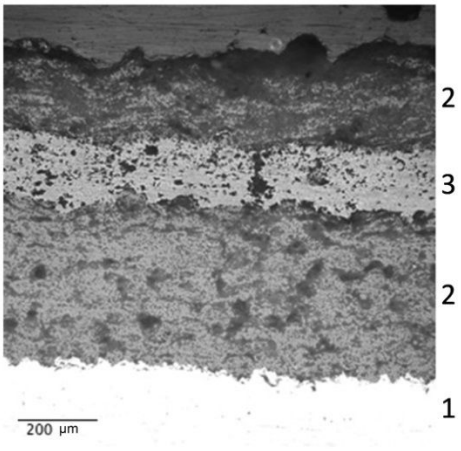


Fig. 5. Microstructure of the three-layer coating of EHE Series No. 2: 1 – steel substrate; 2 – Al_2O_3 layers; 3 – TiO_2 layer. EHE, electric heating element

Analysis of the microstructure of three-layer coatings (Figure 5) showed that the resulting electrical insulating layer between the steel substrate and the electric heating track has a thickness of 400±50 μm and the outer electrical insulating layer has a thickness of 200±30 μm. The resistive tracks formed from TiO_2 have a uniform thickness of 150±50 μm, with the presence of porosity in the coating structure within 10%–13%. The average porosity of the electrical insulating coatings of Al_2O_3 was 20%–25%.

The electrical strength of the electrically insulating Al_2O_3 layer with a thickness of 400±100 μm was 2.5 kV·mm^{-1}. Thus, the Al_2O_3 coating provides the required electrical insulating properties [19].

TiO_2 resistive coatings and the properties of their heating capability were evaluated on a sample of Series No. 1, since it did not have an external protective electrically insulating layer of the Al_2O_3 coating, which made it possible to measure the temperature of the resistive track directly on its surface. Applying 250 V AC to the EHE current-carrying contacts resulted in a maximum current of 0.3 A, which corresponds to a maximum EHE power of 75 W. The distribution of heat over the EHE was measured using the IRISYS 1020 device (Figure 6).

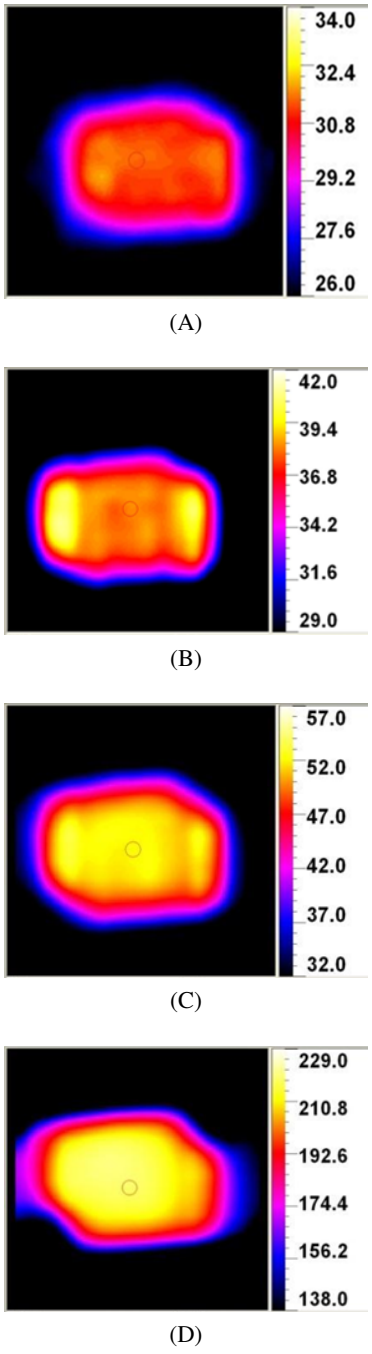


Fig. 6. Temperature distribution along the electric heating track depending on the heating time; at the beginning of the process (**A**); every next 35 s (**B**, **C**); after 100 s (**D**)

The initial temperature of the EHE was 26°C (Figure 6A), and after applying power for 100 s, the temperature reached >200°C (Figure 6D). During the entire time of the experiment, the grad-

ual heating of the electric heating tracks and their heat exchange with the working surface were observed. Initially, heating occurred in the places of current-carrying contacts (Figure 6B), which indicated that these local areas had the greatest resistance. Further, the heating spread over the entire surface of the EHE (Figure 6C). When the temperature reached >230°C, due to the high density of the electric current, overheating and destruction of the local areas of the coating followed, and the electric heating track lost its electrical conductivity. The reason for this phenomenon could be the presence of a large concentration of pores in this area or the presence of cracks, as observed by Bobzin et al. [25] for temperature distribution on thermally sprayed electric heating coatings.

The results of the experiment to determine the influence of the MPS parameters on the CTE of the TiO_2 powders are shown in Table 4.

As a result of the mathematical processing of the experimental data given in Table 4, the regression Eq. (5) for CTE was obtained:

$$\mathrm{CTE} = 15.75 + 1.45I + 0.35G_{\mathrm{pl}} - 0.394H + 7.5P_{\mathrm{pow}}. \quad (5)$$

The coefficients in regression Eq. (5) were calculated by assigning the corresponding units of measure if required: 15.75; 1.45 A^{-1}; 0.35 $slpm^{-1}$; -0.394 mm^{-1}; and 7.5 $min{\cdot}g^{-1}$. The comparison of the calculated and experimental results shows good agreement (Table 4), which indicates the adequacy of the regression model used. Thus, the resulting regression Eq. (5) makes it possible to evaluate the influence of each MPS parameter on the CTE value.

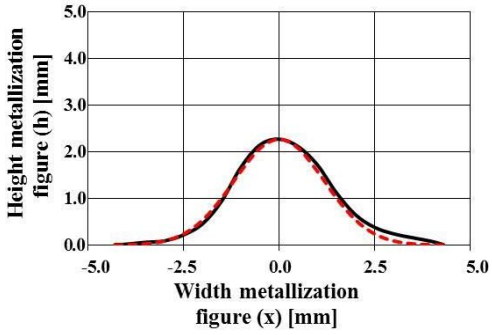
The MPS parameters and the results of the experiment on measuring the geometric dimensions of the metallization figure formed from TiO_2 are shown in Table 5. For this experiment, the spraying distances in all eight runs were increased within the variational deviations compared to the distances presented in Table 4, to prevent overheating of the coating due to the use of a stationary plasmatron.

It was found that the spray spot from the TiO_2 powder has the shape of an ellipse with axes ranging in size from 6 mm to 9.2 mm, where the smaller axis is directed horizontally and the larger axis is directed vertically. The ratio of the axes can be from 1.01 to 1.47, depending on the combination of MPS parameters in the run. Probably, such a shape of the spray spot is caused by the fact that when powder is supplied using a dispenser (in this case, dispenser MD-004), the powder particles are affected by gravity and are directed perpendicular to the axis of the jet. Since the sizes of the powder particles differ from each other, their masses and aerodynamic resistances differ accordingly; therefore, under the influence of gravity, the particles will penetrate into the jet to different depths in the direction of gravity. Under such conditions, the resulting spray spot will have the shape of an ellipse, the large axis of which is located in the vertical plane, that is, it coincides with the direction of gravity (see Figure 2).

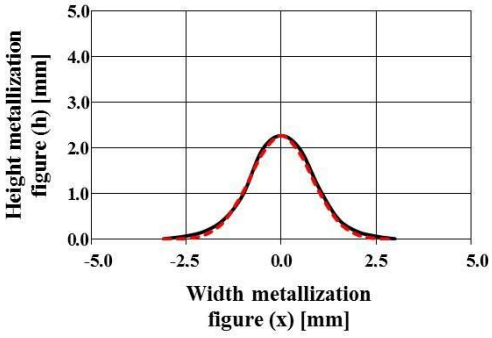
Using the experimental data of measurements of the profiles of metallization figures obtained during MPS (measurements were carried out along the large L and small l axes, see Figure 2), the actual and calculated Gaussian curves were constructed for various spraying parameters (Figure 7); while the coefficient correlations for the calculated and actual curves ranged from 0.9849 to 0.9992, the value of k varied in the range from 0.12 to 0.97.

Thus, it was shown that it is possible to use MPS of TiO_2 powder to form electric heating tracks for the manufacture of EHEs. Electric heating coatings of TiO_2 obtained by the MPS method allow heating the substrate to a temperature of 200°C without loss of the EHE efficiency. An increase in temperature above 230°C leads to local overheating of the track, with loss of electrical conductivity. The temperature limitation and the loss of conductivity are obviously due to the inhomogeneous porous structure of microplasma coatings. In the process of heating TiO_2 coatings in air, the resistance increases in zones with an inhomogeneous coating structure, followed by overheating of the coating and loss of electrical conductivity, as noted earlier by Barabanova et al. [26].

In the process of studying the influence of each MPS parameter on the CTE value, it was found that by selecting the parameters of MPS of electric heat-

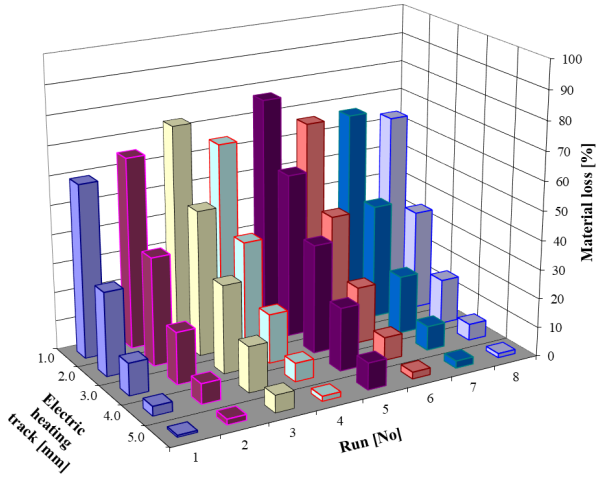


(A)

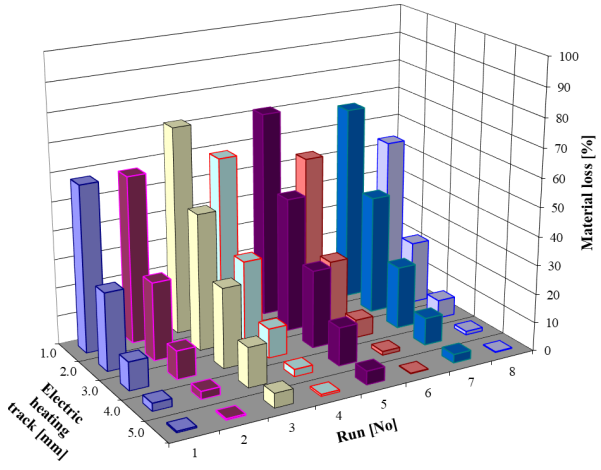


(B)

Fig. 7. Cross section of metallization figures along the spray spot axes (Run 6, Table 5): (**A**) section along the large axis $y = 2.27 \times e^{-0.36x^2}$; (B) section along the small axis $y = 2.27 \times e^{-0.78x^2}$; — graph of the Gaussian distribution (calculated); -- the actual profile of the metallization figure



(A)



(B)

Fig. 8. Losses of the sprayed material associated with the geometric factor depending on the width of the electric heating track: (A) for the large axis L of the spray spot; (B) for the small axis l of the spray spot

ing tracks formed from TiO_2 powder, it is possible to minimize material losses. For example, with an increase in strength of the electric current, the CTE increases due to an increase in the temperature of the plasma jet and a higher heat input into heating the powder particles. This technological parameter (I, A) in the MPS process has the greatest impact on the CTE.

With an increase of the plasma-forming gas flow rate (G_{pl}, slpm), the CTE shows a decrease. This is explained by the fact that with an increase in the gas flow rate, not only does the temperature of the plasma jet decrease, but its velocity also increases. An increase in the velocity of the plasma jet outflow causes an increase in the velocity of particles of the sprayed material, which, in turn, reduces the time they spend in the high-temperature zone of the plasma jet and leads to a decrease in the degree of their heating.

With an increase in the spraying distance (H, mm), a decrease in CTE is observed, which is associated with partial cooling of the sprayed particles and their transition to a solid state when approaching the substrate. From the data on the values of the CTE given in Table 4, it follows that with MPS of TiO_2, the maximum CTE (89%) is achieved in Run 2. Probably, with MPS parameters in Run 2, the energy of the plasma jet makes it possible to

heat the particles to the melting temperature and, at a minimum spray distance (80 mm), to ensure the interaction of molten particles with substrate.

As a result of the calculations performed according to Eq. (3), it was found that the opening angle of the microplasma jet is in the range from 2.0° to 5.2°. The obtained results correspond to the values obtained by Gulyaev et al. [27] for laminar plasma jets.

The results of the calculations of losses of the sprayed material associated with the geometric factor, that is, dependence on the width of the electric heating track, carried out for each run indicated in Table 5, are shown in Figure 8.

Histogram analysis in Figure 8 made it possible to establish that the smallest losses of the sprayed material are ensured when using the parameters in Run 6 (Table 5). Run 6 is characterized by a minimum electric current and a high plasma-forming gas flow rate, which reduces the temperature of the plasma jet and thereby makes it possible to reduce the spray distance without the risk of substrate overheating. Reducing the spray distance, in turn, leads to a decrease in the size of the spray spot. The loss of the sprayed material in this case amounted to 53% when spraying a track with a width of 1.0 mm and was $<1.0\%$ when spraying a track with a width of 5.0 mm.

Thus, MPS technology can find practical application in the manufacture of EHEs to prevent icing of wind turbines, as shown by Gao et al. [28], to protect pipes from freezing, as demonstrated by Yousefzadeh et al. [29], as well as for protecting electric motors and generators from moisture, heating water pumps in winter to prevent their icing, maintaining a constant temperature inside electrical cabinets with automation, heating sliding valves, as well as in the production of special equipment for harsh climatic conditions, where heating of fuels and lubricants in internal combustion engines is required. Based on the obtained results, the authors plan to further optimize the MPS process for the development of a commercial EHE production technology.

4. Conclusions

1. The possibility of obtaining small-sized multilayer EHEs consisting of insulating (Al_2O_3) and electrically conductive (TiO_2) layers by the method of MPS has been experimentally demonstrated, and the temperature range of EHE operability has been estimated. The conductive electric heating layer TiO_2 with a thickness of 150 ± 50 μm and an average porosity of 10% ensures the operation of the EHE with a maximum electric power of 75 W without loss of electrical conductivity when heated from 26°C to 200°C. The electrical insulating strength of the electrically insulating Al_2O_3 layer (thickness 400 ± 50 μm, average porosity 20%) is 2.5 kV·mm^{-2}.
2. It has been established that during MPS of TiO_2 powder, the maximum CTE is 89% at the following MPS parameters: electric current is 45 A, plasma-forming gas flow rate is 120 slpm, spraying distance is 80 mm, and powder feed rate is 0.6 g·min^{-1}. Using regression analysis methods, it was found that the most significant effect on CTE is exerted by the electric current and the plasma-forming gas flow rate (an increase in values leads to better heating of powder particles in the plasma jet).
3. It is shown that, by selecting the parameters of MPS of TiO_2 powder, it is possible to form narrow electric heating tracks and, at the same time, control material losses associated with the size of the sprayed surface. The minimum material loss is achieved at the following MPS parameters: electric current strength of 35 A, plasma-forming gas flow rate of 120 slpm, spraying distance of 100 mm, and powder feed rate of 1.8 g·min^{-1}. The loss is 53% when the track is 1.0 mm wide and $<1.0\%$ when spraying a track with a width of 5.0 mm.

Acknowledgements

The authors express their sincere gratitude to Dr. Victor Glukhovsky of the Department of Non-Destructive Testing of

Welded Joints and Metal Structures, E.O. Paton Electric Welding Institute, for assistance in obtaining some of the results of this study.

References

[1] Yang K, Zhou YZ, Liu M, Song JB, Deng CM. Performance of plasma-sprayed $MoSi_2$-based coating as a heating element. *Ceram Int*. 2020;46(16): 25430–9. doi:10.1016/j.ceramint.2020.07.013.

[2] Bobzin K., Wietheger W., Heinemann H., Schacht A. (2021). $TiOx/Cr_2O_3$ Heating Coatings for Injection Molding of Polyamide. In: *Reisgen, U., Drummer, D., Marschall, H. (eds) Enhanced Material, Parts Optimization and Process Intensification*. EMPOrIA 2020. Lecture Notes in Mechanical Engineering. Springer, Cham. `https://doi.org/10.1007/978-3-030-70332-5_8`

[3] Pashkevich AV, Fedotov AK, Poddenezhny EN, Bliznyuk LA, Fedotova JA, Basov NA, et al. Structure, electric and thermoelectric properties of binary ZnO-based ceramics doped with Fe and Co. *J Alloys Compd*. 2022;895(2): 162621. doi:10.1016/j.jallcom.2021.162621.

[4] Heating Elements Firms ONYX. Available from: `http://onyxmef.narod.ru/nagrev.htm` [Accessed 24th August 2022].

[5] Naghdi S, Rhee KY, Hui D, Park SJ. A review of conductive metal nanomaterials as conductive, transparent, and flexible coatings, thin films, and conductive fillers: different deposition methods and applications. *Coatings*. 2018;8(8): 278. doi:10.3390/coatings8080278.

[6] Zhao Z, Chen H, Liu X, Wang Z, Zhu Y, Zhou Y. The development of electric heating coating with temperature controlling capability for anti-icing/deicing. *Cold Reg Sci Technol*. 2021;184: 103234. doi:10.1016/j.coldregions.2021.103234.

[7] Conze S, Grimm M, Berger L-M, Thiele S, Drehmann R, Lampke T. Influence of simultaneous Cr_2O_3 and TiO_2 additions on the microstructure and properties of APS alumina coatings. *Surf Coat Technol*. 2020;405(15): 126702. doi:10.1016/j.surfcoat.2020.126702.

[8] Scheitz S, Toma F-L, Berger L-M, Puschman R, Sauchuk V, Kusnezoff M. Thermally sprayed multilayer ceramic heating elements. *Therm Spray Bull*. 2011;2: 88–92.

[9] Li X, Yang K, Wang D, Deng C, Zhou Y. Property of TiO_2-$15MgAl_2O_4$ electrical-heating coating prepared by atmospheric plasma spraying and hydrogen heat treatment. *Coatings*. 2020;10: 177. doi:10.3390/coatings10020177.

[10] Vashkevich FF, Spalnik AY, Pluzhko IA. Electrical thermal insulation of inductors for internal heating of tubular blanks. *Constr Mater Sci Mech Eng PGASA*. 2009;48(1): 4–6.

[11] Bobzin K, Wietheger W, Knoch MA, Schacht A. Heating behavior of plasma sprayed TiO_x/Cr_2O_3 coatings for injection molding. *Surf Coat Technol*. 2020;399: 126199. doi:10.1016/j.surfcoat.2020.126199.

[12] Smyth RT, Andersen JC. Production of resistors by arc plasma spraying. *Electrocomponent Sci Technol*. 1975;2: 135–45, Gordon and Breach Science Publishers Limited. doi:10.1155/APEC.2.135.

[13] Hajaligol MR, Fleischhauer GS, Deevi SC, Higgins CT, Hayes PH, Herman H, et al. Tubular heater for use in an electrical smoking article. U.S. Patent 5,665,262. 9th September 1997.

[14] Michels D, Hadeler J, Lienhard VJH. High-heat-flux resistance heaters from VPS and HVOF thermal spraying. *Exp Heat Transf*. 1998;11(4): 341–59. doi:10.1080/08916159808946570.

[15] Prudenziati M, Cirri G, Dal Bo P. Novel high-temperature reliable heaters in plasma spray technology. *J Therm Spray Technol*. 2006;15(3): 329–31. doi:10.1361/105996306x124293.

[16] Zehui Z, Huawei C, Xiaolin L, ZelinlanW, Yantong Z, Yuping Z. The development of electric heating coating with temperature controlling capability for anti-icing/deicing. *Cold Reg Sci Technol*. 2021;184(1–2): 103234. doi:10.1016/j.coldregions.2021.103234.

[17] Rad MR, Bajgiran MM, Moreau C, McDonald A. Fabrication of thermally sprayed coating systems for mitigation of ice accumulation in carbon steel pipes and prevention of pipe bursting. *Surf Coat Technol*. 2020;397: 126013. doi:10.1016/j.surfcoat.2020.126013.

[18] Borisov YuS, Vojnarovich SG, Kislitsa AN, Kalyuzhny SN, Glukhovsky VYu. Application of the method of microplasma spraying for manufacturing resistance heating element. *Paton Weld J*. 2018;2: 33–7. doi:10.15407/tpwj2018.02.07.

[19] AZoNetwork. Titanium Dioxide. Available from: `https://www.azom.com/properties.aspx?ArticleID=1179` [Accessed 24th August 2022].

[20] Bajgiran MM, Rad MR, McDonald A, Moreau C. Microstructure, phase and dielectric strength of thermally sprayed alumina layers in coating-based heating systems. *Int J Appl Ceram Technol*. 2021;18(5): 1–16. doi:10.1111/ijac.13731.

[21] Yushenko K, Borisov Y, Voynarovych S, Fomakin O. Plasmatron for spraying of coatings. Pub. No.:WO/2004/010747, International Application No.: PCT/UA2003/000014, Publication date: 29.01.2004. (IRP4).

[22] Voinarovych SG. Alontseva DL, Khozhanov AR, Krasavin AL, Kyslytsia AN, Kalyuzhny SN. Effect of microplasma spraying parameters on losses of sprayed Zr wire and coating porosity. *Bulletin of KazNU. Phy Ser*. 2021;79(4): 82–96. doi:10.26577/RCPh.2021.v79.i4.10.

[23] ASTM International USA. *Standard test methods for determining area percentage porosity in thermal sprayed coatings*; 2021. p.E2109–01. Available from: Nov 04, 2021 `https://www.astm.org/e2109-01r21.html`

[24] Montgomery DC, Runger GC, Hubele NR. *Engineering Statistics*. 5th ed. Hoboken: John Wiley and Sons Inc;

2015.

[25] Bobzin K, Öte M, Knoch MA, Alkhasli I. Temperature distribution on thermally sprayed heating conductor coatings. In: *IOP Conference: Materials Science and Engineering*. 21st Chemnitz Seminar on Materials Engineering, 6–7 March 2019 (Germany);480(1): 11. doi:10.1088/1757-899X/480/1/012002.

[26] Barabanova EV, Zaborovsky KM, Posadova EM, Castro RA. Effect of porosity on electrophysical properties of PZT ceramics. In: *Proceedings of the Russian State Pedagogical University. A.I. Herzen*. 2013;157: 79–83. doi:10.1088/1757-899X/49/1/012026.

[27] Gulyaev IP, Kuzmin VI, Golubev MP, Tyryshkin PA, Dolmatov AV. Visualization of the gas-dynamic structure of plasma flows of the deposition plasma torch "PNK-50" by the shadow method. *Bull Yugra State Univ*. 2018;4(51): 61–8. doi:10.17816/byusu20180461-68.

[28] Gao L, Ma L, Liu Y, Hu H. A novel heating-coating hybrid strategy for wind turbine icing mitigation. In: *International Conference on Icing of Aircraft, Engines, and Structures*, 10 June 2019, USA. doi:10.4271/2019-01-2029.

[29] Yousefzadeh Z, Rad MR, McDonald A, Lloyd SM. Life cycle assessment of a thermal sprayed Al2O3-NiCr resistive heating coating for pipe freeze protection. *J Therm Spray Technol*. 2022;31(2): 378–95. doi:10.1007/s11666-021-01308-6.

Received 2022-11-23
Accepted 2023-01-30